Stochastic 3D modeling of three-phase microstructures with fully connected phases

Jakub Staněk

Charles University in Prague, Department of Mathematics Education

joint work with

Matthias Neumann, Omar Pecho, Lorenz Holzer,
Viktor Beneš and Volker Schmidt

August 27, 2015

Motivation

Experimental image data gained by FIB- tomography of Ni-YSZ anode occuring in solid oxide fuel cells

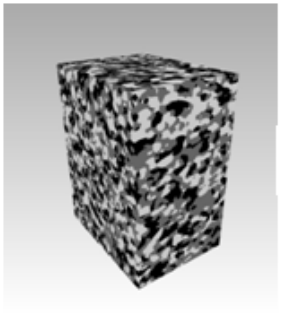

25.5 µm

Parametric stochastic microstructure model

Model parameters control

Virtual three phase microstructures (all phases are completely connected)

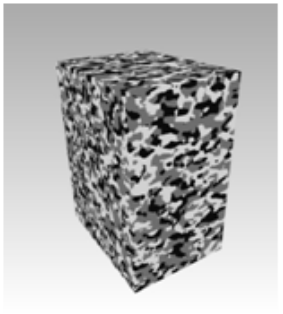

Geometrical characteristics
- Volume fractions of phases
- Surface area of phases
- Length of tripple phase boundary
- Chordlength distribution

Physical properties
- effective conductivity
- area specific resistance

The combination of stochastic modeling and FE simulations generates a large database for an investigation of the relationship between geometrical characteristics and physical properties of such Ni-YSZ anodes

Stochastic microstructure model

1. Modeling idea
   - Model step 1: Start with three random point patterns in a set $W = [0, w_1] \times [0, w_2] \times [0, w_3]$, where $w_1, w_2, w_3 > 0$.
   - Model step 2: Modeling of three random connected geometric graphs
   - Model step 3: Three phases are modeled such that each graph is contained in the corresponding phase
2. Aim: Flexible model with respect to
   - volume fraction of phases
   - length of TPB
   - geodesic tortuosity
   - constrictivity (microstructure characteristic describing bottleneck effects)

Microstructure characteristics

Consider the three phases: pores, YSZ and Ni phase as a stationary random closed sets denoted by Ξ_1, Ξ_2, Ξ_3, respectively.

Volume fractions p_i

The volume fraction of Ξ_i is defined by

$$p_i = \mathbb{E}v_3(\Xi_i \cap W)/v_3(W),$$

where v_d denotes a d-dimensional Legesgue measure.

Triple phase boundary *tpb*

The length of triple phase boundary per unit volume is defined as

$$tpb = \mathbb{E}\mathcal{H}_1(\Xi_1 \cap \Xi_2 \cap \Xi_3 \cap [0,1]^3),$$

where $\mathcal{H}_d$ denotes a $d-$dimensional Hausdorff measure.

Microstructure characteristics

mean geodetic tortuosity $\tau_{i,W}$

Denote $W_I = \{(x_1, x_2, x_3) \in W : x_1 = 0\}$, $W_O = \{(x_1, x_2, x_3) \in W : x_1 = w_1\}$ and l the lenght of the shortest path from a given point $x \in W_I$ to the opposite side W_O through the $i-$th phase Ξ_i.

Mean geodesic tortuosity $\tau_{i,W}$ is the expectation of the mean value of $\frac{l}{w_1}$ over all possible start points

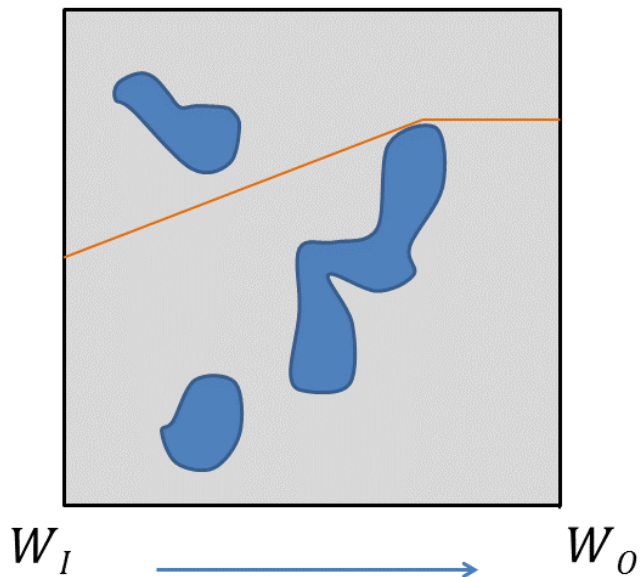

$2D$-visualization of the shortest path in Ξ_i, represented in gray, from W_I to W_O.

Microstructure characteristics

mean geodesic tortuosity $\tau_{i,W}$

Denote:

- $\mathcal{P}_{\Xi_i}(A,B) = \{\eta : [0,1] \to \Xi_i \text{ } \textit{continuous} : \eta[0] \in A, \eta[1] \in B\}$ the set of all path from a set $A \subset \mathbb{R}$ to a set $B \subset \mathbb{R}$ going through the phase Ξ_i,
- $L(\eta)$ the Euclidean lenght of a path $\in \mathcal{P}_{\Xi_i}(A,B)$,
- $W_{I,i} = \{x \in W_I : \mathcal{P}_{\Xi_i}(\{x\}, W_O) \neq \emptyset\}$ the set of all points W_I from which a path to W_O through Ξ_i exists.

Mean geodesic tortuosity is defined as

$$\tau_{i,W} = \mathbb{E}\left(\frac{1}{w_1 \mathcal{H}_2(W_{I,i})} \int_{W_{I,i}} \min_{\eta \in \mathcal{P}(\{x\}, W_O)} L(\eta) d\mathcal{H}_2(x)\right).$$

Microstructure characteristics

Constrictivity factor $\beta_{i,W}$

$$\beta_{i,W} = \left(\frac{r_{min,i}}{r_{max,i}} \right)^2$$

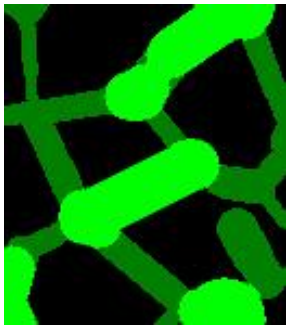

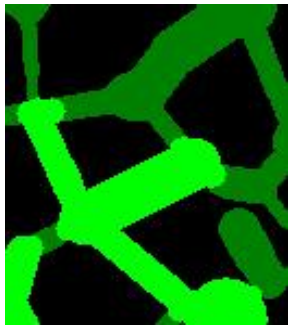

$r_{max,i}$ is the maximal radius r such that in expectation at least 50% of the i-th phase can be covered by spheres of radius r, which are completely contained in the i-th phase.

$r_{min,i}$ is the maximal radius r such that in expectation at least 50% of the i-th phase can be filled by an intrusion of spheres with radius r in transport direction.

Microstructure characteristics

Constrictivity factor $\beta_{i,W}$

Denote:

- $\overline{B}(o,r)$ the closed ball centered at the origin with radius $r > 0$,
- $op_r(A) = (A \ominus \overline{B}(o,r)) \oplus \overline{B}(o,r)$ the opening of the set A with $\overline{B}(o,r)$, where $\ominus$ and $\oplus$ denote erosion and dilation, respectively,
- $F_{\Xi_i,W}(r) = \{x \in (\Xi_i \ominus \overline{B}(o,r)) \cap W : \mathcal{P}_{\Xi_i \ominus \overline{B}(o,r)}(W_I, \{x\}) \neq \emptyset\}$ the larger subset of $(\Xi_i \ominus \overline{B}(o,r)) \cap W$ which is connected to W_I.

Define

$$r_{\max,i} = \sup\{r \geq 0 : 2\mathbb{E}v_3(op_r(\Xi_i) \cap W) \geq \mathbb{E}v_3(\Xi_i \cap W)\},$$

$$r_{\min,i} = \sup\{r \geq 0 : 2\mathbb{E}v_3(F_{\Xi_i,W}(r) \oplus \overline{B}(o,r)) \geq \mathbb{E}v_3(\Xi_i \cap W)\}$$

and

$$\beta_{i,W} = \left(\frac{r_{min,i}}{r_{max,i}}\right)^2.$$

Model step 1 - Poisson point processes

- Model is defined in $\mathbb{R}^3$. For simulation we use a rectangular cuboid W as observation window.
- Let X_i, $i = 1, 2, 3$, be independent homogeneous Poisson point processes with intensities $\lambda_i > 0$.

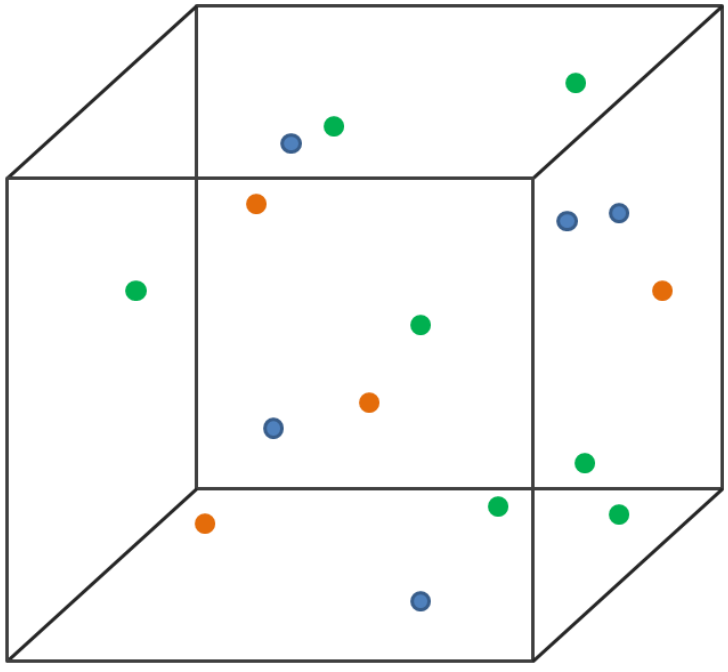

Model step 2 - Beta skeletons

$G_i = (X_i, E_i)$, $i = 1, 2, 3$ random geometric graphs, where the edge sets are formed by β-skeletons.

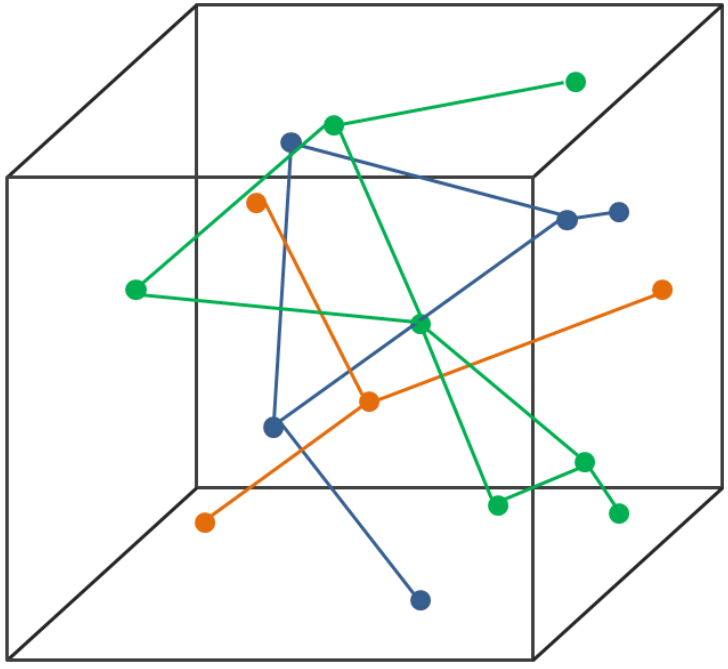

Model step 2 - Beta skeletons

Formal definition

Let $b \geq 1$, $i \in \{1, 2, 3\}$ and x, y be points of X_i. Denote the open ball centered at $x \in \mathbb{R}^3$ with radius $r > 0$ by $B(x, r)$. Define

$$A_b(x, y) = B(m_{x,y}^{(1)}, |m_{x,y}^{(1)} - y|) \cap B(m_{x,y}^{(2)}, |m_{x,y}^{(2)} - x|),$$

with

$$m_{x,y}^{(1)} = \frac{b}{2}x + \left(1 - \frac{b}{2}\right)y,$$

$$m_{x,y}^{(2)} = \frac{b}{2}y + \left(1 - \frac{b}{2}\right)x.$$

Then, x and y are connected by an edge in the beta skeleton $G_b(X_i) = (X_i, E_b)$ if $A_b(x, y)$ contains no third point of X_i.

$b = 1$

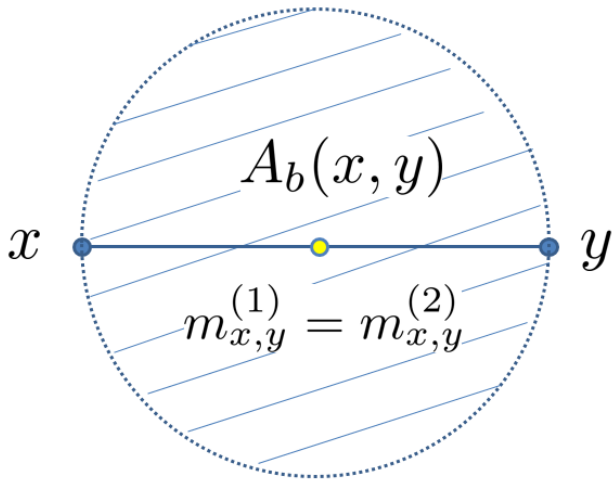

Model step 2 - Beta skeletons

Formal definition

Let $b \geq 1$, $i \in \{1, 2, 3\}$ and x, y be points of X_i. Denote the open ball centered at $x \in \mathbb{R}^3$ with radius $r > 0$ by $B(x, r)$. Define

$$A_b(x, y) = B(m_{x,y}^{(1)}, |m_{x,y}^{(1)} - y|) \cap B(m_{x,y}^{(2)}, |m_{x,y}^{(2)} - x|),$$

with

$$m_{x,y}^{(1)} = \frac{b}{2}x + \left(1 - \frac{b}{2}\right)y,$$

$$m_{x,y}^{(2)} = \frac{b}{2}y + \left(1 - \frac{b}{2}\right)x.$$

Then, x and y are connected by an edge in the beta skeleton $G_b(X_i) = (X_i, E_b)$ if $A_b(x, y)$ contains no third point of X_i.

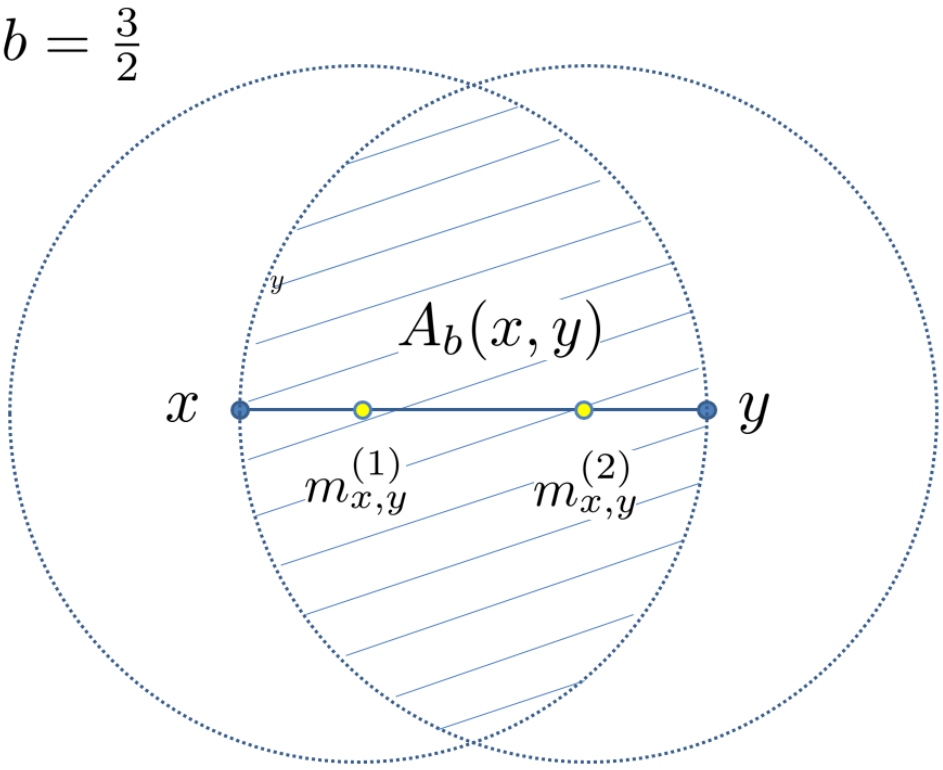

Model step 2 - Beta skeletons

Formal definition

Let $b \geq 1$, $i \in \{1, 2, 3\}$ and x, y be points of X_i. Denote the open ball centered at $x \in \mathbb{R}^3$ with radius $r > 0$ by $B(x, r)$. Define

$$A_b(x, y) = B(m_{x,y}^{(1)}, |m_{x,y}^{(1)} - y|) \cap B(m_{x,y}^{(2)}, |m_{x,y}^{(2)} - x|),$$

with

$$m_{x,y}^{(1)} = \frac{b}{2}x + \left(1 - \frac{b}{2}\right) y,$$

$$m_{x,y}^{(2)} = \frac{b}{2}y + \left(1 - \frac{b}{2}\right) x.$$

Then, x and y are connected by an edge in the beta skeleton $G_b(X_i) = (X_i, E_b)$ if $A_b(x, y)$ contains no third point of X_i.

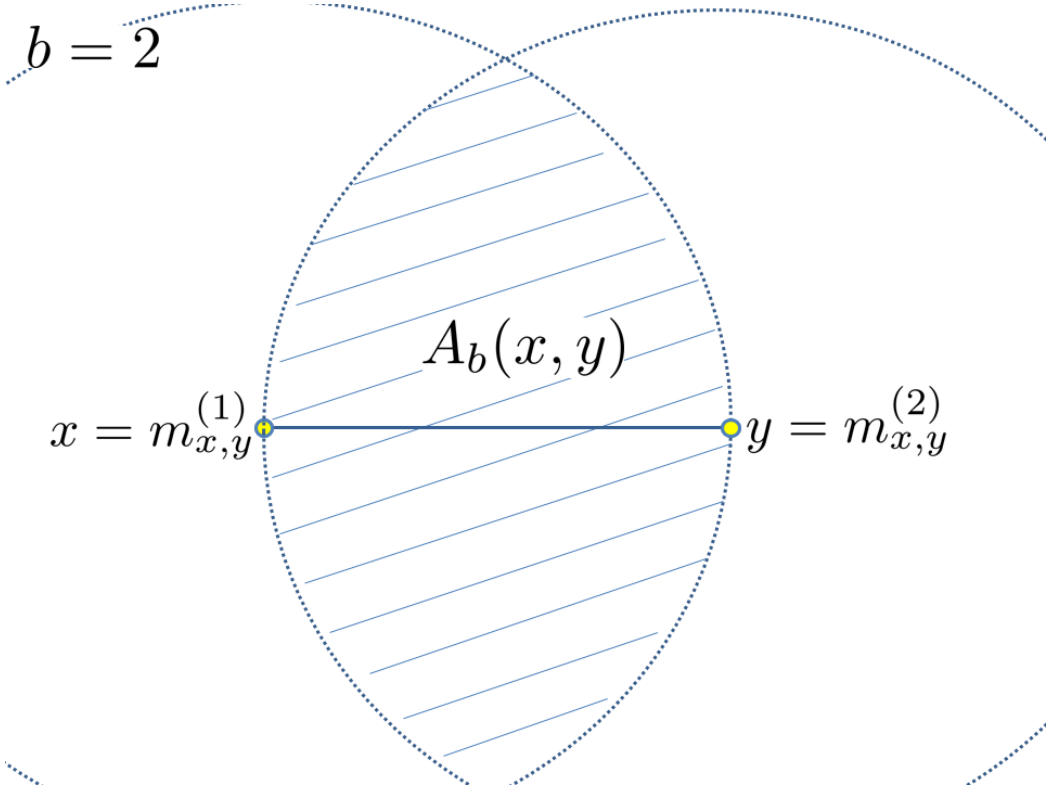

Model step 2 - Beta skeletons

Properties of the beta-skeleton

- With increasing b the connectivity in the beta-skeleton decreases.
- For $b \in [1, 2]$, the beta-skeleton of a Poisson point process is completely connected with probability 1.

  See Hirsch et al., Advances in Applied Probability, 45 (2013), 20-36

Model step 3

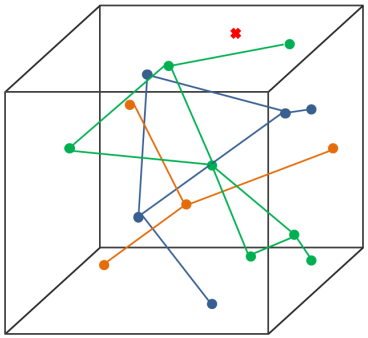

- Ξ_1 ... pores,
- Ξ_2 ... YSZ-phase,
- Ξ_3 ... Ni-phase.

Denote the obtained beta-skeletons by G_1, G_2, G_3. The three phases are defined by random closed sets Ξ_i, $i = 1, 2, 3$, such that

$$x \in \Xi_i \Leftrightarrow d(x, G_i) \leq \min_{j \neq i} d(x, G_j),$$

where $d(x, G_i)$ is the minimal distance of x to the graph G_i.

Proposition1

Let $d \in \mathbb{N}$, $b \in [1,2]$ and X be a Poisson process in $\mathbb{R}^d$ with intensity $\lambda > 0$. Let $G_b(X) = (X, E_b)$ be the beta sceleton on X with parameter b. Then the expected edge length $e_{\lambda,b} = \frac{1}{2}\mathbb{E}\sum^{\neq}_{x_i,x_j \in X} \mathcal{H}_1([x_i, x_j] \cap [0,1]^d)$ of $G_b(X)$ in $[0,1]^d$ is given by

$$e_{\lambda,b} = \frac{2^{d+1-\frac{1}{d}}\lambda^{1-\frac{1}{d}}\pi^{\frac{1}{2d}}}{b^{d+1}\int_0^{arccos(1-\frac{1}{b})}\sin^d(t)dt}\frac{\Gamma(\frac{d+1}{2})\Gamma(\frac{1}{d})}{\Gamma(\frac{d}{2}+1)},$$

where Γ denotes the gamma function. For $d = 3$ we get

$$e_{\lambda,b} = 8\Gamma\left(\frac{4}{3}\right)\sqrt[3]{\frac{6\lambda^2}{\pi(3b-1)^4}}.$$

The volume fraction of phases can be predicted by a function of the parameters $\lambda_1, \lambda_2, \lambda_3, b_1, b_2, b_3$ using a linear regresion model.

$$\hat{p}_i = 0.9132 \frac{e_{\lambda_i, b_i}}{e_{\lambda_1, b_1} + e_{\lambda_2, b_2} + e_{\lambda_3, b_3}} + 0,0292 + \epsilon_1,$$

where $\epsilon_1 \sim N(0, 0.013^2)$. The coefficient determination $R^2 = 0.99$

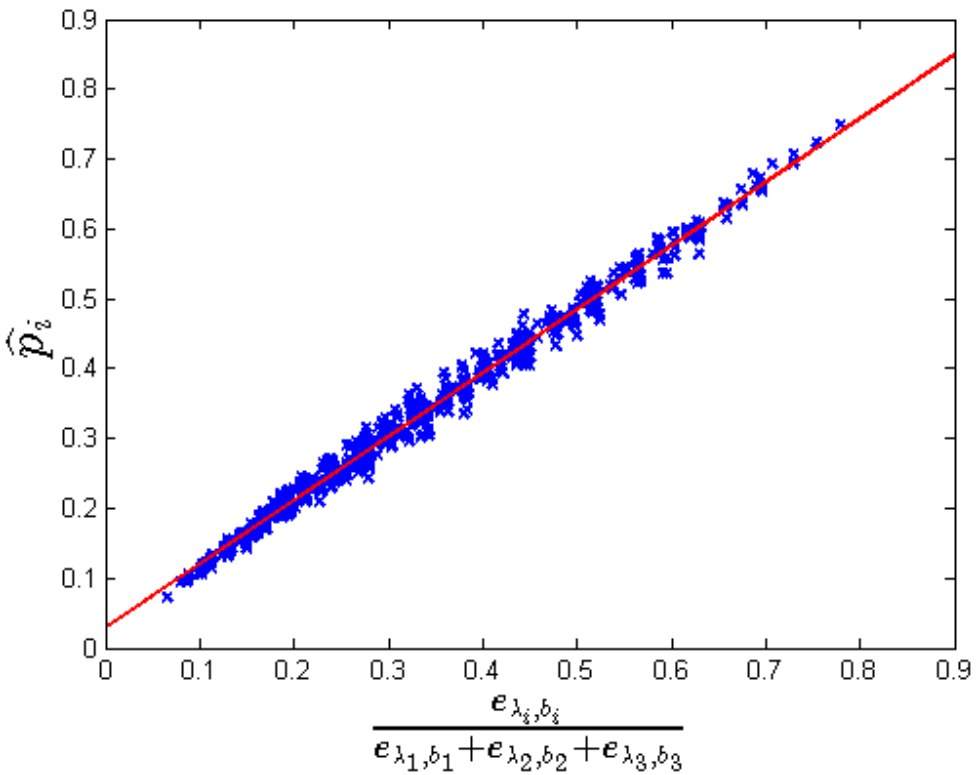

The relationship between model parametes and volume fraction allow us to reduce the number of free parameters in the model under the condition that the volume fractions p_1, p_2 and p_3 are fixed. For a given volume fraction and given model parameters λ_1, b_1, b_2, b_3 it holds

$$p_j^n = -0.02929 + 1.10349 p_j \approx \frac{\sqrt[3]{\frac{6\lambda_j^2}{(3\beta_j - 1)^4}}}{\sqrt[3]{\frac{6\lambda_1^2}{(3\beta_1 - 1)^4}} + \sqrt[3]{\frac{6\lambda_2^2}{(3\beta_2 - 1)^4}} + \sqrt[3]{\frac{6\lambda_3^2}{(3\beta_3 - 1)^4}}}$$

$$\Downarrow$$

$$\frac{p_i^n}{p_j^n} \approx \sqrt[3]{\frac{\lambda_i^2 (3\beta_j - 1)^4}{\lambda_j^2 (3\beta_i - 1)^4}}$$

$$\Downarrow$$

$$\lambda_i \approx \lambda_1 \cdot \left(\frac{-0.02929 + 1.10349 p_i}{-0.02929 + 1.10349 p_1} \right)^{\frac{3}{2}} \cdot \left(\frac{3\beta_i - 1}{3\beta_1 - 1} \right)^2$$

for $i = 2, 3$.

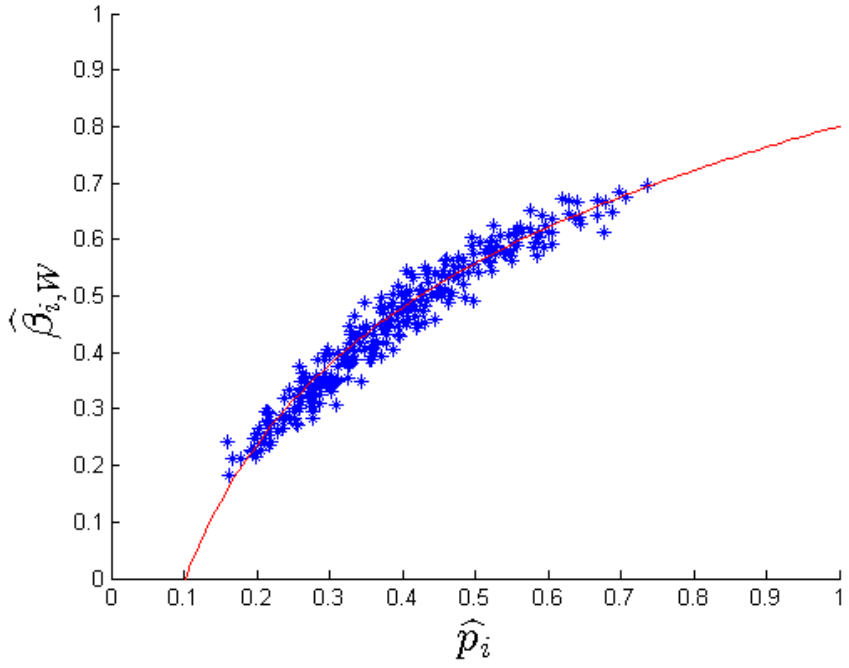

Relationship between volume fractions and constrictivity factors. We can observe, that model is not flexible with respect to constrictivity since there is a strong correlation between volume fraction and constrictivity factor of the same phase. The correlation can be modeled by

$$\hat{\beta}_{i,W} = 0.35 \log \hat{p}_i + 0.8 + \epsilon_2$$

with $\epsilon_2 \sim N(0, 0.028^2)$.

Model step 3

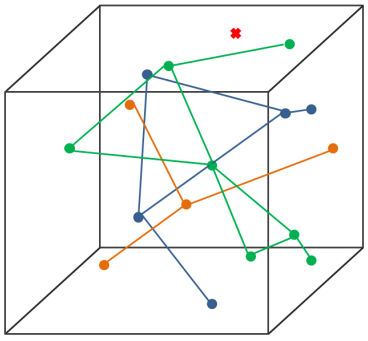

- Ξ_1 ... pores,
- Ξ_2 ... YSZ-phase,
- Ξ_3 ... Ni-phase.

Let $\gamma_1, \gamma_2, \gamma_3 \geq 1$. Denote the obtained beta-skeletons by G_1, G_2, G_3. The three phases are defined by random closed sets Ξ_i, $i = 1, 2, 3$, such that

$$x \in \Xi_i \Leftrightarrow d'^{i}_{\gamma}(x, G_i) \leq \min_{j \neq i} d'_{\gamma_j}(x, G_j),$$

where

$$d'_{\gamma_i}(x, G_i) = \min\{\gamma_i d(x, G_i), d(x, X_i)\}.$$

Here $d(x, X_i)$ is the minimal distance of x to the set of vertices X_i and $d(x, G_i)$ is the minimal distance of x to the graph G_i.

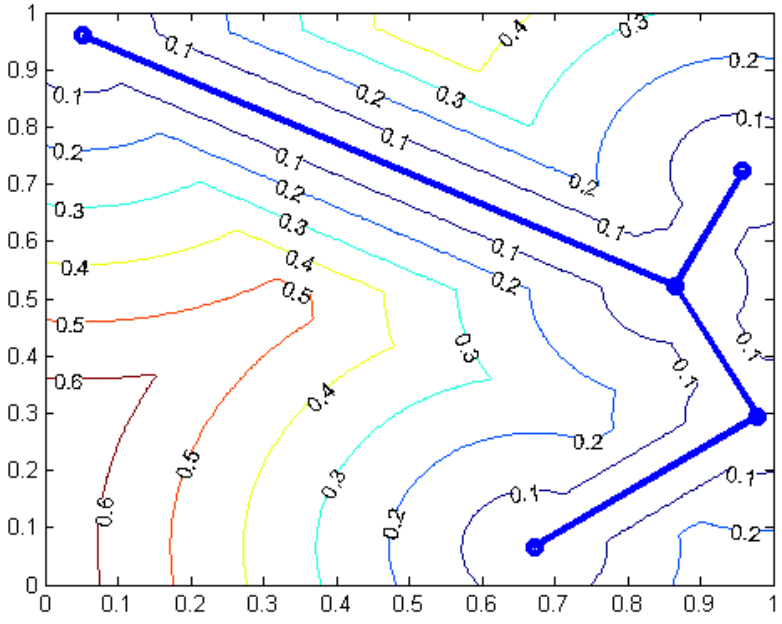

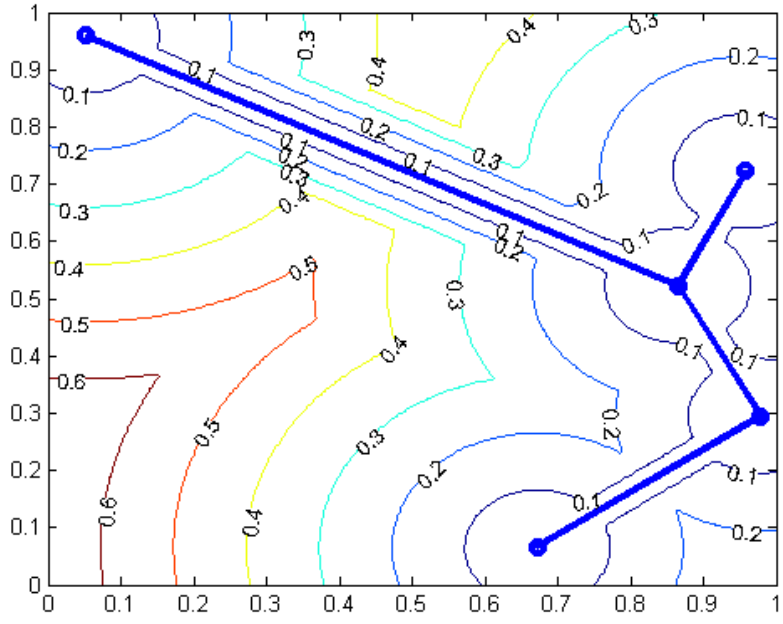

Visualization of the contour lines of the distance to a given graph represented in blue with respect to d'_γ. The parameter γ is 2 on the left and 4 on the right.

Comparing model to the data

The following fit to experimental image data is obtained by the Nelder-Mead method:

	p_2	p_3	$\tau_{2,W}$	$\tau_{3,W}$	$\beta_{2,W}$	$\beta_{3,W}$	tpb
Image data	0.42	0.32	1.13	1.19	0.41	0.29	0.0033
Simulation	0.40	0.32	1.11	1.14	0.42	0.33	0.0036
Relative error	0.05	0.00	0.02	0.04	0.02	0.14	0.09

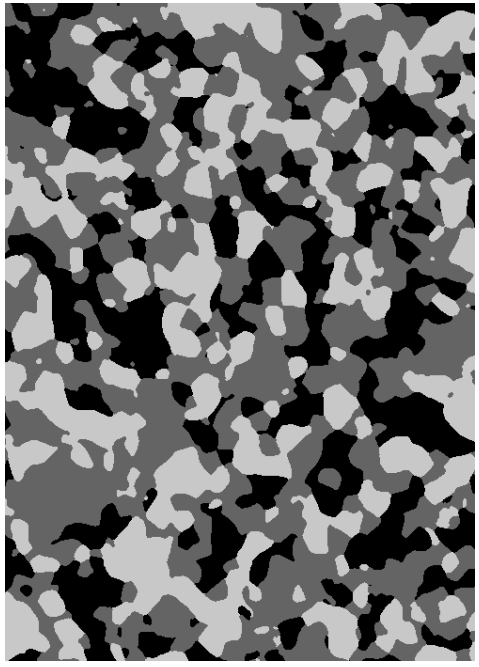

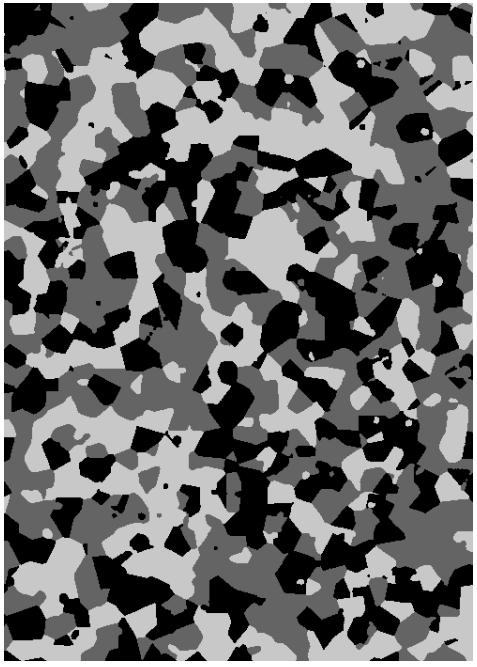

2D slices of experimental (left) and virtual (right) microstructures

Fitted parameters

Fitted data by Nelder-Mead method with cost function

$$3\sum_{i=2}^{3}\frac{|\hat{p}_{i,sim}-p_i|}{p_i}+2\sum_{i=2}^{3}\frac{|\hat{\beta}_{i,sim}-\beta_i|}{\beta_i}+$$
$$+2\sum_{i=2}^{3}\frac{|\hat{\tau}_{i,sim}-\tau_i|}{\tau_i}+\frac{|\hat{tpb}_{sim}-tpb|}{tpb}.$$

Parameters	Fitted values
λ_1	$29.3\mu m^{-3}$
λ_2	$39.9\mu m^{-3}$
λ_3	$32.2\mu m^{-3}$
b_1	2.11
b_2	1.97
b_3	1.94
γ_1	4.47
γ_2	4.31
γ_3	4.12

References

G. Gaiselmann, M. Neumann, O. Pecho, T. Hocker, L. Holzer, and V. Schmidt (2014): Quantitative relationships between microstructure and effective transport properties based on virtual materials testing. *AIChE Journal 60*, 1983–1999.

L. Holzer, B. Iwanschitz, T. Hocker, L. Keller, O. Pecho, G. Sartoris, P. Gasser, and B. Muench (2013): Redox cycling of Ni–YSZ anodes for solid oxide fuel cells: Influence of tortuosity, constriction and percolation factors on the effective transport properties. *Journal of Power Sources 242*, 179–194.

C. Hirsch, D. Neuhaeuser, and V. Schmidt (2013): Connectivity of random geometric graphs related to minimal spanning forests. *Advances in Applied Probability 45*, 289–298.